

# Harmonic analysis and field quality improvement of an HTS quadrupole magnet for a heavy ion accelerator

Zhan Zhang<sup>a</sup>, Shaoqing Wei<sup>a</sup>, Sangjin Lee<sup>\*,a</sup>, Hyun Chul Jo<sup>b</sup>, Do Gyun Kim<sup>b</sup>, and Jongwon Kim<sup>b</sup>

<sup>a</sup> Uiduk University, Gyeongju, Korea

<sup>b</sup> Rare Isotope Science Project, Institute for Basic Science, Korea

(Received 9 May 2016; revised or reviewed 26 June 2016; accepted 27 June 2016)

## Abstract

In recent years, the iron-dominated high-temperature superconductor (HTS) quadrupole magnets are being developed for heavy ion accelerators. Field analyses for iron-dominated quadrupole magnets were based on the normal-conducting (NC) quadrupole magnet early in the development for accelerators. Some conclusions are still in use today. However, the magnetic field of iron-dominated HTS quadrupole magnets cannot fully follow these conclusions. This study established an HTS quadrupole magnet model and an NC quadrupole magnet model, respectively. The harmonic characteristics of two magnets were analyzed and compared. According to the comparison, the conventional iron-dominated quadrupole magnets can be designed for maximum field gradient; the HTS quadrupole magnet, however, should be considered with varying field gradient. Finally, the HTS quadrupole magnet was designed for the changing field gradient. The field quality of the design was improved comparing with the result of the previous study. The new design for the HTS quadrupole magnet has been suggested.

*Keywords* : Heavy ion accelerator, HTS quadrupole magnets, Harmonic analysis, iron-dominated quadrupole magnets

## 1. INTRODUCTION

Iron-dominated quadrupole magnets used for beam transport are components of accelerator systems [1]. In a heavy ion accelerator, the quadrupole magnets have to withstand radiation and accommodate high heat loads. High-temperature superconductor (HTS) quadrupole magnets are suitable for the application in such an environment [2]. Therefore, the use of an HTS quadrupole magnet in a heavy ion accelerator is suggested. In quadrupole magnets, the  $2\varphi$  (4-pole) component is the main magnetic field, and the field inhomogeneity is composed of the  $6\varphi$  (12-pole) component, the  $10\varphi$  (20-pole) component, and so on. The field quality of a quadrupole magnet is expressed by using higher-order components (order  $> 2$ ) with respect to the  $2\varphi$  component in a good field region [3-6]. In the case of conventional iron-dominated quadrupole magnet, the harmonic components were analyzed for the maximum field gradient to check the field quality, because the maximum values of harmonic components were considered at maximum field gradient. In the author's past study, the iron-induced field and the coil-induced field of the iron-dominated HTS quadrupole magnet have been analyzed separately [7]. In this study, a conventional normal-conducting (NC) quadrupole magnet and an HTS quadrupole magnet were analyzed in this way and compared to show that the conventional method is not suitable for the HTS quadrupole magnet. To improve the field quality, this study designed the HTS quadrupole magnet for varying field gradients using the evolution

strategy (ES) method [8] Comparing with the design based on conventional method, the field harmonic components were reduced, and a better design for the HTS quadrupole magnet was put forward.

## 2. THEORY

Based on the solution of the Laplace equation in a cylindrical coordinate system, the magnetic flux density can be expressed as [3]:

$$B_{\rho}(\rho, \varphi, z) = \sum_{n=0}^{\infty} B_{\rho n}(\rho, z) \sin(n\varphi)$$
$$B_{\varphi}(\rho, \varphi, z) = \sum_{n=0}^{\infty} B_{\varphi n}(\rho, z) \cos(n\varphi) \quad (1)$$

where  $\rho$  is the radius,  $\varphi$  is the azimuthal angle,  $z$  is the coordinate in the longitudinal direction, and  $n$  is a non-negative integer for harmonic components.  $B_{\rho}$  and  $B_{\varphi}$  are the magnetic flux densities in the radial and the azimuthal direction, respectively.  $B_{\rho n}$  and  $B_{\varphi n}$  are the multipole field components of  $B_{\rho}$  and  $B_{\varphi}$ , respectively.

Because  $2\varphi$  component is the main magnetic field, relative multipole harmonic components  $b_{\rho n}$  and  $b_{\varphi n}$  can be defined as  $b_{\rho n} = B_{\rho n}/B_{\rho 2}$  and  $b_{\varphi n} = B_{\varphi n}/B_{\varphi 2}$ , which are in units of  $10^{-4}$  [9] to express the field quality. In three-dimensional analysis, the relative multipole components are integrated as  $b_{\rho n} = \int B_{\rho n} dz / \int B_{\rho 2} dz$  and  $b_{\varphi n} = \int B_{\varphi n} dz / \int B_{\varphi 2} dz$ . The effective length of the focusing area  $L_{\text{eff}}$  is expressed as  $L_{\text{eff}} = \int B_{\rho 2}(z) dz / B_{\rho 2}(z=0)$  [10].

The total magnetic field  $B$  can be separated into the

\* Corresponding author: sjlee@uu.ac.kr

coil-induced magnetic field  $B_s$  and the iron-induced magnetic field  $B_c$  as  $B = B_s + B_c$  [5]. For the field component,  $B_{\rho n} = B_{s\rho n} + B_{c\rho n}$  and  $B_{\varphi n} = B_{s\varphi n} + B_{c\varphi n}$ , where  $B_{s\rho n}$  and  $B_{s\varphi n}$  are the multipole field component induced by the coil and  $B_{c\rho n}$  and  $B_{c\varphi n}$  are the multipole field component induced by the iron core.  $\int B_{s\rho n} dz / L_{\text{eff}}$ ,  $\int B_{c\rho n} dz / L_{\text{eff}}$ ,  $\int B_{s\varphi n} dz / L_{\text{eff}}$ ,  $\int B_{c\varphi n} dz / L_{\text{eff}}$ ,  $\int B_{sn} dz / L_{\text{eff}}$  and  $\int B_{cn} dz / L_{\text{eff}}$  were defined as the effective multipole field harmonic components through quadrupole magnets in longitudinal direction.

To check the harmonics of an iron-dominated quadrupole magnet, the six effective multipole field components were considered at the same time.

### 3. ANALYSIS

#### 3.1. An NC Quadrupole Magnet Model

The NC quadrupole magnet consists of an iron yoke and four NC coils [11]. Fig. 1(a) shows the geometry of the 1/8 iron yoke. The length of the yoke is 200 mm. Fig. 1(b) and 1(c) show the sizes of one NC coil. There are four coils for the whole magnet. One coil is constructed with 46 turns of wires in which there is a cooling channel whose diameter is 5 mm. The NC quadrupole magnet is operated under the conditions  $G \leq 19.8$  T/m with  $\rho_0 = 30.5$  mm, and  $L_{\text{eff}} \geq 230$  mm, where  $G$  is the field gradient, which is the  $2\varphi$  component relative to the reference radius  $\rho_0$ . The operating current,  $I_{op}$  is 160 A. The maximum current density is  $3.6$  A/mm<sup>2</sup> [11].

Based on the symmetry of the quadrupole magnet, a 1/16 model was created with the MagNet<sup>TM</sup> program for a three-dimensional simulation. The effective multipole field components for  $2\varphi$ ,  $6\varphi$ , and  $10\varphi$  were checked with respect to  $I_{op}$ . In Fig. 2(a), the ratio of iron-induced field by the main field,  $r_c$  is defined as  $r_c = B_{c\rho 2} / B_{\rho 2} \times 100\%$ . The ratio of iron-induced field,  $r_c$  is always greater than 95%. Therefore, this magnet is an iron-dominated magnet. Fig. 2(b) shows the coil-induced component  $\int B_{s\rho 6} dz / L_{\text{eff}}$  is very little, and can be ignored.  $\int B_{c\rho 6} dz / L_{\text{eff}}$  and  $\int B_{\rho 6} dz / L_{\text{eff}}$  are almost same and increased monotonously with respect to the operating

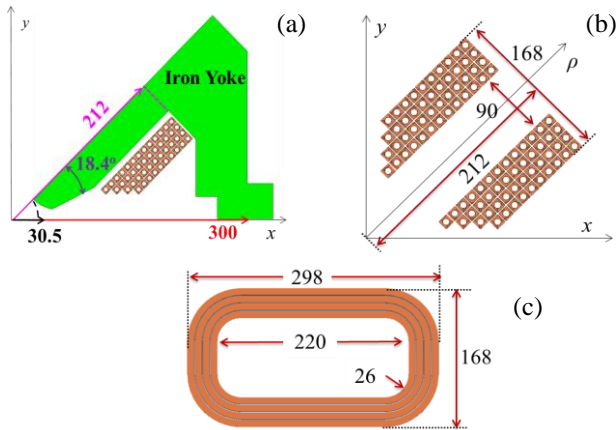


Fig. 1. Structure of the NC quadrupole magnet: (a) section view of 1/8 iron yoke, (b) section view of one coil, (c) size coil winding.

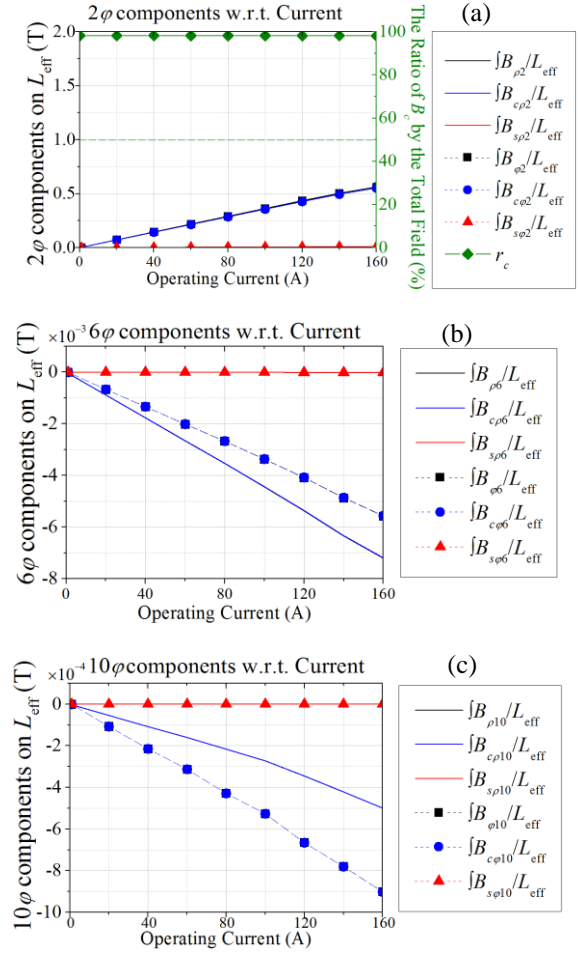


Fig. 2. Effective field harmonic components for the NC quadrupole magnet: (a)  $2\varphi$  components, (b)  $6\varphi$  components, (c)  $10\varphi$  components.

current. The  $6\varphi$  components always achieve the maximum value with maximum operating current. Fig. 2(c) shows that the  $10\varphi$  components have the same effect as the  $6\varphi$  components. Therefore, the field quality of an NC quadrupole magnet can be expressed using the harmonics with maximum field gradient or maximum operating current. During the design of the NC quadrupole magnets, only the maximum field gradient is considered.

#### 3.2. An HTS Quadrupole Magnet Model

The HTS quadrupole magnet is constructed by an iron yoke and four racetrack coils. Fig. 3(a) shows the geometry of the 1/8 iron yoke. Four double pancake (DPC) HTS coils are used for the whole magnet. Fig. 3(b) shows the chamfer of the yoke. The sizes of the inner winding and outer winding of one DPC HTS coil are shown in Fig. 3(c) and 3(d), respectively. Table I shows the description and the value of design parameters. The HTS quadrupole magnet is operated under the conditions  $G \leq 9$  T/m with  $\rho_0 = 150$  mm, and  $L_{\text{eff}} \geq 580$  mm [4].

Fig. 4(a) shows that the ratio of the iron-induced field is always greater than 50%. Therefore, this magnet is also an iron-dominated magnet. However,  $r_c$  is much less than the case of NC quadrupole magnet. Fig. 4(b) shows that the

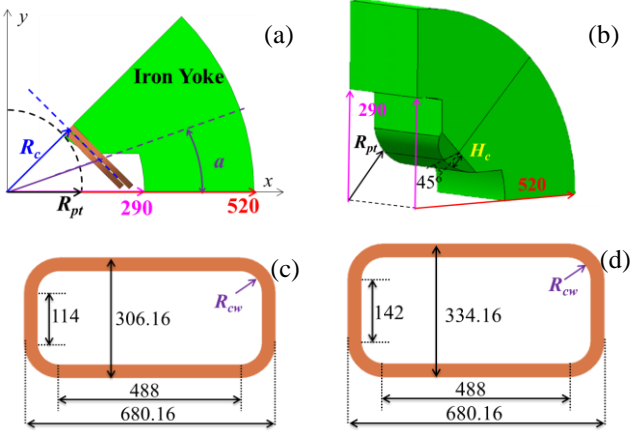


Fig. 3. Structure of the HTC quadrupole magnet: (a) section view of the 1/8 iron yoke, (b) chamfer in 1/8 iron yoke, (c) size of the inner winding, and (d) size of the outer winding.

TABLE I  
DESIGN PARAMETERS OF THE HTC QUADRUPOLE MAGNET.

| Item                              | Symbol   | Value  |
|-----------------------------------|----------|--------|
| Pole tip radius(mm)               | $R_{pt}$ | 168    |
| Radius of coil(mm)                | $R_c$    | 173.83 |
| Angle of cutting pole( $^\circ$ ) | $a$      | 24     |
| The height of the chamfer(mm)     | $H_c$    | 0      |
| Radius of corner of windings(mm)  | $R_{cw}$ | 60     |

$\int B_{\rho 6} dz / L_{\text{eff}}$  can achieve the maximum value when  $I_{op} \approx 200$  A. Both of the absolute values of  $\int B_{cp6} dz / L_{\text{eff}}$  and  $\int B_{sp6} dz / L_{\text{eff}}$  are increased monotonously with respect to the operating current, however, they have opposite signs. Therefore,  $\int B_{\rho 6} dz / L_{\text{eff}}$  does not increase monotonously with operating current. Fig. 4(c) shows that the  $10\phi$  components can achieve the maximum value when  $I_{op} \approx 300$  A. Because the HTS quadrupole magnet has a larger reference radius, the harmonics have to be checked to  $22\phi$  components. Fig. 4(d), Fig. 4(e), and Fig. 4(f) show  $14\phi$ ,  $18\phi$ , and  $22\phi$  components, respectively. Each harmonic obtained the maximum value with different operating currents.

According to the analysis for two kinds of quadrupole magnets, we can know that: For NC quadrupole magnets, the iron-induced field comprises a large proportion of the total field. Therefore, all the harmonic components always achieve their maximum values with maximum operating current or maximum field gradient. For HTS quadrupole magnets, the iron-induced field is dominating but the coil-induced field cannot be ignored. In addition, the maximum value of each component appears at different operating current.

#### 4. DESIGN

The previous study [4] designed the HTS quadrupole magnet for maximum field gradient which was based on the harmonic characteristics of NC magnets. This study presents a design of HTS quadrupole magnet by varying the field gradient and compared the design with the previous study.

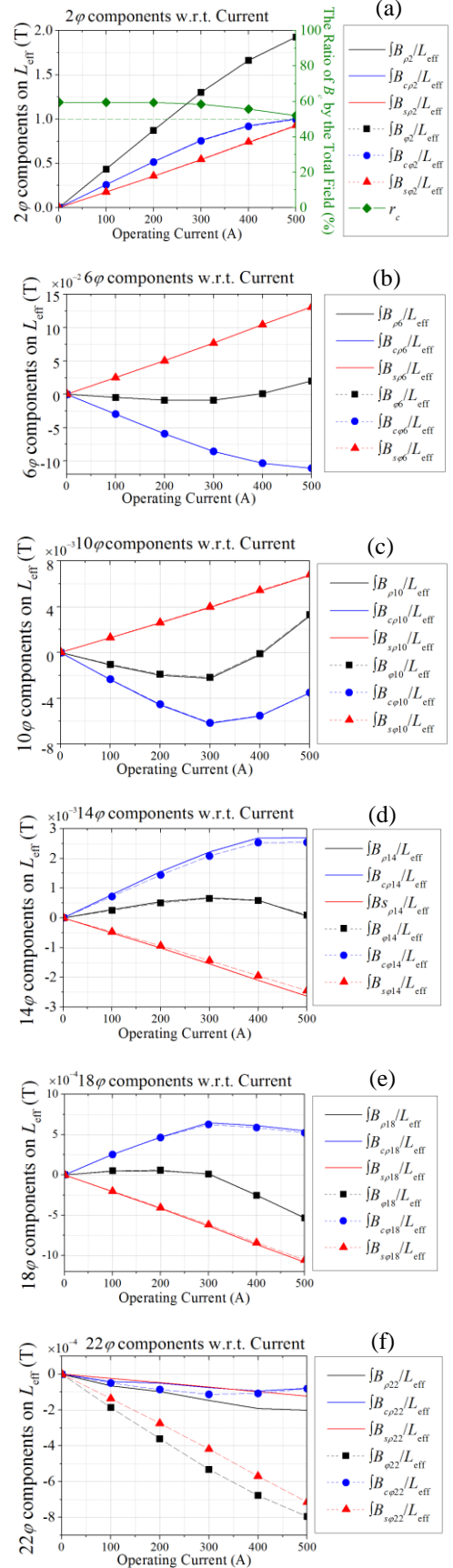


Fig. 4. Effective field harmonic components for the HTS quadrupole magnet: (a)  $2\phi$  components, (b)  $6\phi$  components, (c)  $10\phi$  components, (d)  $14\phi$  components, (e)  $18\phi$  components, (f)  $22\phi$  components.

The constraints for the design process are expressed as:

$$\begin{aligned} G &\geq 9 \text{ T when } I_{op} = 320 \text{ A} \\ L_{eff} &\geq 580 \text{ mm} \end{aligned} \quad (2)$$

According to [4], the design parameters were selected as:

$$\mathbf{x} = [R_{pt}, R_c, \alpha, H_c, R_{cw}]^T \quad (3)$$

The suggested object function with respect to current is expressed as:

$$OF = \frac{1}{10} \sum_{k=1}^5 w_k \frac{\int_0^{I_{max}} |b_{\rho(2+4k)}| dI + \int_0^{I_{max}} |b_{\varphi(2+4k)}| dI}{I_{max}} \quad (4)$$

where  $I_{max}$  is the maximum value of operating current,  $k$  is an integer from 1 to 5, and  $w_k$  is the weight value for each harmonic component. This study fixes  $w_k$  as 1.

The values of design parameters are shown in Table II. Table II also presents the object function values of previous design and the presented design. With less object function, the design in this study is better for the HTS quadrupole magnet.

Table III and IV present in detail the relative harmonic components of two designs with respect to the current. The previous design can only achieve less harmonic component with the maximum operating current. The presented design, however, can achieve better values except in the case of the maximum operating current. According to the comparison, the field quality of the presented design is considered better than that of previous design. Therefore, the field quality was improved.

TABLE II  
COMPARISON BETWEEN DIFFERENT MODELS.

| Parameter     | Initial Design       | Previous Design       | Presented Design    |
|---------------|----------------------|-----------------------|---------------------|
| $x$           | [168 173.83 24 0 60] | [168.5 179 20.5 0 55] | [168 178.5 19 1 60] |
| $OF(10^{-4})$ | 25.51                | 7.68                  | 3.54                |

TABLE III  
RELATIVE HARMONIC COMPONENTS FOR  
PREVIOUS DESIGN IN UNITS OF  $10^{-4}$ .

|     | $I_{op}=60\text{A}$ | $I_{op}=120\text{A}$ | $I_{op}=180\text{A}$ | $I_{op}=240\text{A}$ | $I_{op}=300\text{A}$ |
|-----|---------------------|----------------------|----------------------|----------------------|----------------------|
| $n$ | $G=1.74\text{T/m}$  | $G=3.48\text{T/m}$   | $G=5.22\text{T/m}$   | $G=6.96\text{T/m}$   | $G=8.63\text{T/m}$   |
|     | $b_{pn}$            | $b_{pn}$             | $b_{pn}$             | $b_{pn}$             | $b_{pn}$             |
| 6   | -35.7749            | -35.769              | -35.7159             | -25.2868             | -5.33041             |
| 10  | -5.25679            | -5.24925             | -5.23659             | -3.3579              | -1.20254             |
| 14  | -4.61503            | -4.61476             | -4.61499             | -4.70036             | -4.68345             |
| 18  | 0.324108            | 0.323415             | 0.321866             | 0.147084             | 0.037874             |
| 22  | -0.18305            | -0.18234             | -0.18152             | -0.07875             | -0.14383             |

TABLE IV  
RELATIVE HARMONIC COMPONENTS FOR  
PRESENTED DESIGN IN UNITS OF  $10^{-4}$ .

|     | $I_{op}=60\text{A}$ | $I_{op}=120\text{A}$ | $I_{op}=180\text{A}$ | $I_{op}=240\text{A}$ | $I_{op}=300\text{A}$ |
|-----|---------------------|----------------------|----------------------|----------------------|----------------------|
| $n$ | $G=1.75\text{T/m}$  | $G=3.51\text{T/m}$   | $G=5.26\text{T/m}$   | $G=7.00\text{T/m}$   | $G=8.70\text{T/m}$   |
|     | $b_{pn}$            | $b_{pn}$             | $b_{pn}$             | $b_{pn}$             | $b_{pn}$             |
| 6   | -2.84962            | -2.8493              | -1.64794             | 6.659845             | 25.57637             |
| 10  | 0.754453            | 0.764341             | 2.273801             | 2.856963             | 4.329756             |
| 14  | -5.26882            | -5.27233             | -5.94749             | -6.06382             | -6.10587             |
| 18  | -1.58564            | -1.58357             | -1.2172              | -1.18186             | -1.23044             |
| 22  | 0.662096            | 0.660331             | 0.432417             | 0.363601             | 0.313197             |

## 5. CONCLUSION

In case of NC quadrupole magnets, the iron-induced field is much greater than the coil-induced field. The maximum value of each component always appears at the maximum operating current. Therefore, the NC quadrupole magnet can be designed for maximum field gradient using the iron pole surface optimization to improve the iron-induced field components [11].

In case of HTS quadrupole magnets, the coil-induced field components cannot be neglected and the maximum value of each component is located at different operating currents. The existing method in [11] cannot be used to solve the design problem for HTS quadrupole magnets. Because the coil-induced field components aren't related with the pole surface. This paper described the particular characteristics HTS quadrupole magnets and presented suitable design method using these characteristics. Finally, the field quality of the HTS quadrupole magnet can be enhanced and a better design result has been suggested

## ACKNOWLEDGMENT

This work was supported by the Rare Isotope Science Project of Institute for Basic Science funded by Ministry of Science, ICT and Future Planning and National Research Foundation of Korea (2013M7A1A1075764).

## REFERENCES

- [1] Jack Tanabe, "Iron Dominated Electromagnets-Design, Fabrication, Assembly and Measurements," SLAC-R-754, June 2005.
- [2] J. P. Cozzolino *et al.*, "Engineering Design of HTS Quadrupole for FRIB," *Accelerator Technology, Proceedings of Particle Accelerator Conference*, New York, USA, 2011.
- [3] H. Takeda *et al.*, "Extraction of 3D field maps of magnetic multipoles from 2D surface measurements with applications to the optics calculations of the large-acceptance superconducting fragment separator BigRIPS," *Nuclear Instruments and Methods in Physics*, Research B317, pp. 798–809, 2013.
- [4] Zhan Zhang, Sangjin Lee *et al.*, "A Study on the Optimization of an HTS Quadrupole Magnet System for a Heavy Ion Accelerator Through Evolution Strategy," *IEEE Trans. Appl. Supercond.*, vol. 26, pp. 1–4, 2016.
- [5] A. Kalimov and P. Nalimov, "Optimization of the Pole Shape of Quadrupole Magnets by MULTIMAG," *IEEE Trans. App. Supercond.*, vol.16, pp. 1282, 2006.
- [6] J. P. Cozzolino *et al.*, "Engineering Design of HTS Quadrupole For FRIB," *Accelerator Technology, TUP162, Proceedings of Particle Accelerator Conference*, New York, USA, 2011.
- [7] Z. Zhang, S. Lee and H. Jo *et al.*, "Magnetic Field characteristics from HTS Quadrupole Magnet of In-Flight Separator for a Heavy Ion Accelerator," *Superconductivity and Cryogenics*, vol. 17, no. 3, pp. 23–27, 2015.
- [8] N. Hansen, *The CMA Evolution Strategy: A Tutorial*, ArXiv e-prints, arXiv:1604.00772, 2016.
- [9] S. Russenschuck, *Field Computation for Accelerator Magnets*. Weinheim, Germany: Wiley-VCH, 2010.
- [10] J. J. Murray, "Effective Length Measurement for Quadrupole Magnets," SLAC-TN-63-010, 1963.
- [11] D. Einfeld, "Specifications, quality control, manufacturing, and testing of accelerator magnets," CELLS-ALBA, Barcelona, Spain. Available: <http://arxiv.org/ftp/arxiv/papers/1103/1103.1815.pdf>.